

Preparatory studies for a high-precision Penning-trap measurement of the ^{163}Ho electron capture Q -value

F. Schneider^{1,2,a}, T. Beyer³, K. Blaum³, M. Block^{1,4,5}, S. Chenmarev^{3,6}, H. Dorrer^{1,7,8}, Ch.E. Düllmann^{1,4,5,9}, K. Eberhardt^{1,5}, M. Eibach^{3,b}, S. Eliseev³, J. Grund^{1,9}, U. Köster¹⁰, Sz. Nagy³, Yu.N. Novikov^{3,6}, D. Renisch¹, A. Türlér^{7,8}, and K. Wendt^{2,9}

¹ Institut für Kernchemie, Johannes Gutenberg-Universität, 55128 Mainz, Germany

² Institut für Physik, Johannes Gutenberg-Universität, 55128 Mainz, Germany

³ Max-Planck-Institut für Kernphysik, 69117 Heidelberg, Germany

⁴ GSI Helmholtzzentrum für Schwerionenforschung GmbH, 64291 Darmstadt, Germany

⁵ Helmholtz-Institut Mainz, 55099 Mainz, Germany

⁶ Physical Faculty, Saint Petersburg State University, 199034 Saint Petersburg, Russia

⁷ Paul Scherrer Institute, 5232 Villigen, Switzerland

⁸ Universität Bern, 3012 Bern, Switzerland

⁹ PRISMA Cluster of Excellence, Johannes Gutenberg-Universität, 55099 Mainz, Germany

¹⁰ Institut Laue-Langevin, 38000 Grenoble, France

Received: 6 March 2015 / Revised: 3 June 2015

Published online: 22 July 2015 – © Società Italiana di Fisica / Springer-Verlag 2015

Communicated by P. Salabura

Abstract. The ECHo Collaboration (Electron Capture ^{163}Ho) aims to investigate the calorimetric spectrum following the electron capture decay of ^{163}Ho to determine the mass of the electron neutrino. The size of the neutrino mass is reflected in the endpoint region of the spectrum, *i.e.*, the last few eV below the transition energy. To check for systematic uncertainties, an independent determination of this transition energy, the Q -value, is mandatory. Using the TRIGA-TRAP setup, we demonstrate the feasibility of performing this measurement by Penning-trap mass spectrometry. With the currently available, purified ^{163}Ho sample and an improved laser ablation *mini-RFQ* ion source, we were able to perform direct mass measurements of ^{163}Ho and ^{163}Dy with a sample size of less than 10^{17} atoms. The measurements were carried out by determining the ratio of the cyclotron frequencies of the two isotopes to those of carbon cluster ions using the time-of-flight ion cyclotron resonance method. The obtained mass excess values are $ME(^{163}\text{Ho}) = -66379.3(9)$ keV and $ME(^{163}\text{Dy}) = -66381.7(8)$ keV. In addition, the Q -value was measured for the first time by Penning-trap mass spectrometry to be $Q = 2.5(7)$ keV.

1 Introduction

The masses of the neutrinos are among the still unknown quantities in the Standard Model. From the observation of neutrino oscillations it is known that at least two of the flavors are required to be massive. Since then a strong thrive to determine the neutrino mass scale has begun. And so far the most stringent limit on the mass of the electron antineutrino of $m(\bar{\nu}_e) < 2.05$ eV (95% C.L.) has been determined by two high-precision MAC-E filters in Mainz [1] and Troitsk [2]. In both cases, the energy spectrum of electrons emitted in the ^3H β -decay near its high-energy endpoint was analyzed. The experience from these

studies led to the design of the next-generation electron spectrometer neutrino mass experiment KATRIN, which aims for a sensitivity limit below 0.2 eV (90% C.L.) [3].

A closely related approach regarding the physics involved, which significantly differs in the spectroscopy and detection method involved, is the investigation and analysis of an electron capture decay for the determination of the mass of the electron neutrino $m(\nu_e)$. A suitable candidate would be ^{163}Ho , which decays to ^{163}Dy with the lowest known electron capture Q -value and a half-life of 4570 years making a calorimetric measurement well feasible [4].

In β decay processes the energy is shared between the emitted electron and the neutrino, leading to a continuous energy spectrum for the electrons. In contrast, in electron capture the energy of the emitted neutrino is given by the Q -value after subtracting the excitation energy of the

^a e-mail: Fabian.Schneider@uni-mainz.de

^b Current address: National Superconducting Cyclotron Laboratory, Michigan State University, 48824 East Lansing, Michigan, USA.

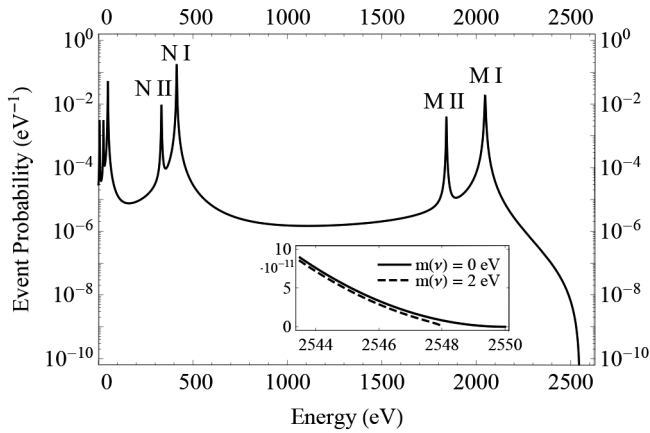


Fig. 1. Calculated calorimetric spectrum of the ^{163}Ho electron capture for a Q -value of 2.550 keV and a zero neutrino mass. The resonances originate from capture of electrons from the shells as indicated. Note the logarithmic scale. Inset: Detailed view of the endpoint region showing the spectrum for two different assumed neutrino masses.

daughter atom with one or more holes and an additional electron in the outer shell. To reach the ground state, the daughter atom releases the excitation energy via emission of Auger electrons and X-rays. Accordingly, in a calorimetric measurement, where all the energy emitted in the decay minus the part taken away by the neutrino is measured, the energy spectrum is characterized by several strong resonances each of them corresponding to the energy of the discrete excitations in the daughter atom. Thus, the spectrum is the sum of the corresponding Breit-Wigner resonances at energies E_i with widths Γ_i multiplied by the phase space term, which depends on the Q -value and the neutrino mass:

$$\frac{\delta W}{\delta E} \propto (Q - E) \sqrt{(Q - E)^2 - m_\nu^2} \cdot \sum_i \frac{\lambda_i \cdot \Gamma_i / 2\pi}{(E - E_i)^2 + \Gamma_i^2 / 4}. \quad (1)$$

The strength of the individual resonances, λ_i , is calculated from theory and includes as most relevant terms the square of the electron wave function at the nucleus, occupation probabilities, nuclear matrix elements, and corrections for the wave function overlap between initial and final atomic states [5]. Due to the small energy available for the decay of ^{163}Ho , only captures from the 3s shell and beyond are allowed. More detailed descriptions include two- and three-hole states, introducing small satellite peaks to the spectrum [6, 7]. Figure 1 shows an electron capture spectrum of ^{163}Ho calculated using one-hole states, based on the recommended Q -value [8] and the atomic parameters as reported in [9]. In the inset, the effect of a finite neutrino mass $m(\nu_e) = 2\text{ eV}$ at the end point region of the spectrum is shown compared to the case of a massless neutrino. Once again, as in the case of β decay, the strongest influence of the neutrino mass on the shape of the spectrum appears at the endpoint. However, there is a minor influence extending over the

complete spectrum, which modifies the strengths of the resonances. This was used in previous calorimetric measurements to determine the Q -value and assign a limit to the neutrino mass in a single measurement. The highest sensitivity has been achieved by Springer *et al.* [10], who were able to determine a limit of $m(\nu_e) \leq 225\text{ eV}$ and a Q -value of 2.561(20) keV. Similar measurements with different detection techniques lead to the currently recommended Q -value of 2.555(16) keV [8] but could not lower the limit on the neutrino mass. However, not all Q -value measurements are in agreement, with a grouping of several complementary results around 2.8 keV with uncertainties well below 100 eV is observed [11, 12].

The novel approach of the ECHo Collaboration (Electron Capture ^{163}Ho [13]) to determine $m(\nu_e)$ is to analyze the endpoint region of the ^{163}Ho electron capture spectrum with high-resolution cryogenic calorimeters. In this energy region, the spectrum is dominated by the term $(Q - E) \sqrt{(Q - E)^2 - m_\nu^2}$ [4], reducing the influence of theoretical uncertainties. A sensitivity for the neutrino mass of 10 eV is aimed for in the first stage of the experiment. A subsequent goal of the ECHo Collaboration is to develop a large scale experiment able to reach sub-eV sensitivity. A very important parameter for the determination of the electron neutrino mass is the energy available to the decay, the Q -value. This quantity can be extracted from the analysis of the calorimetrically measured spectrum, while for the elimination of systematic uncertainties, such as, *e.g.*, shifts from atomic and solid state physics effects, an independent measurement is of utmost importance. Penning-trap mass spectrometry offers the required precision and accuracy to measure Q independently [14]. However, the required relative mass uncertainty of 10^{-11} for ^{163}Ho and ^{163}Dy is attainable only with dedicated ultra-high-precision experiments as, *e.g.*, PENTATRIP [15, 16] or FSU trap [17]. Penning-trap facilities with lower precision, *e.g.*, TRIGA-TRAP, can yet contribute with preparatory studies. As ^{163}Ho is not readily available, the suitability of the sample produced by the ECHo Collaboration in regard of purity and chemical behavior is of high concern for the measurements. Additionally, an ion source capable of reliably producing pulses of a few or even single ions without significant isobaric contaminations is needed for most Penning-trap experiments. Finally, a measurement of the atomic masses with an uncertainty below 1 keV can already serve as a new anchor point for the nuclear mass landscape as presented in the atomic mass evaluation [8]. There, the smallest uncertainties in the area of $140 \leq A \leq 180$ are around 1.6 to 2.0 keV, even for stable nuclides.

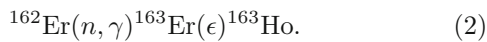
2 Experiment

The Penning-trap mass spectrometer TRIGA-TRAP is part of the TRIGA-SPEC setup at the Institute of Nuclear Chemistry in Mainz, Germany. TRIGA-SPEC comprises two radioactive ion beam experiments coupled to a fissionable target, which is installed in closest proximity to

the core of the research reactor TRIGA Mainz. Alternatively, off-line ion sources provide beams of stable [18,19] or long-lived radionuclides, like ^{163}Ho or transuranium isotopes [20]. Overall scientific goal of the TRIGA-SPEC experiment is the investigation of nuclear ground state properties with Penning-trap mass spectrometry and collinear laser spectroscopy [21].

2.1 Sample preparation

As the radioisotope ^{163}Ho does not occur naturally, it must be produced artificially by one of several possible production methods. Only two of them are promising to fulfill the high demands with respect to sample size and purity connected with neutrino mass measurements: neutron irradiation of ^{162}Er [22] or proton irradiation of ^{nat}Dy [23]. For the ECHO experiment, neutron irradiation is the method of choice. The available sample was produced in a collaborative European effort by the Paul Scherrer-Institute (Villigen, CH), the Institut Laue-Langevin (Grenoble, FR), and the Universities of Mainz and Heidelberg in Germany. The production mechanism is neutron capture of ^{162}Er and subsequent electron capture decay:



30 mg of erbium, enriched to 20% in ^{162}Er , were chemically processed to remove any lanthanide contaminants lighter than erbium, then irradiated in the high-flux reactor at the Institut Laue-Langevin at a neutron flux of $1.3 \cdot 10^{15} \text{ cm}^{-2} \text{ s}^{-1}$ [24] for about 50 days. Nevertheless, undesired reaction pathways occur, starting from other erbium isotopes as well as residual contaminants present in the feed stock. These lead to the production of stable as well as long-lived radioactive contaminations in the sample, primarily thulium isotopes and ^{165}Ho , as well as minor amounts of ^{166m}Ho . After a cooling period of four months, holmium was isolated from the heavier lanthanide elements by means of ion extraction chromatography. The final sample contained about $1.6 \cdot 10^{18}$ atoms of ^{163}Ho . No further radioisotopes besides ^{166m}Ho were detected in γ -spectrometry studies. The largest stable contamination, with about 10% abundance with respect to ^{163}Ho , are the remnants of the erbium feed stock. Whereas ^{166m}Ho would cause an increased background in the calorimetric spectrum, it is of no relevance for the Penning-trap measurements, as TRIGA-TRAP employs mass-selective buffer-gas cooling as high-resolution mass separation technique [25]. Thus, only isobaric species may enter the trap together with the isotope of interest and induce unwanted and perturbing shifts in the measured cyclotron frequency. The only stable, non-molecular isobar of ^{163}Ho present in the sample is ^{163}Dy . It was already contained with less than 0.2% Dy by mass in the erbium feed stock, as commercially available lanthanide samples generally contain traces of other lanthanides, but was quantitatively removed in the chemical purification performed before irradiation. ^{163}Dy is also generated by the decay of ^{163}Ho and

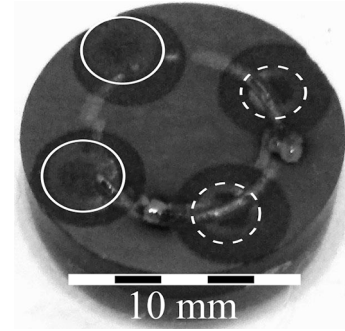


Fig. 2. Photograph of the used laser ablation target. The superimposed circles mark the positions of the sample spots, ^{163}Ho (solid line) and ^{nat}Dy (dashed line). Also visible is the laser trace produced by rotating the target under the laser spot around an offset rotation axis.

via (n,p) reactions on ^{163}Ho in the reactor during irradiation. The use of ion extraction chromatography after irradiation removed these remnants. To verify the purity, the sample was analyzed by resonance ionization mass spectrometry and neutron activation analysis. Both results indicate no dysprosium contamination above 1% with respect to the ^{163}Ho content in the sample. From the full sample, a small fraction was transferred to a nitric acid solution to be deposited on the laser ablation target.

The sample used as ^{163}Dy source, was dysprosium nitrate with natural isotopic composition, *i.e.*, a 24.9% ^{163}Dy content. No ^{163}Ho was expected to be present in this sample, which was thus used without chemical treatment. Both solutions were pipetted two times on the target surface, each drop containing $3 \cdot 10^{16}$ atoms of either ^{163}Ho or ^{163}Dy . The target was a 2 mm thick disc with 14 mm diameter made out of Sigradur, a commercial, glass-like carbon material, on which four sample positions were prepared by sandblasting, as depicted in fig. 2. The roughened surface changes the laser desorption behavior to a more sustained pattern, *i.e.*, a lower ion yield per laser pulse for a larger number of pulses.

2.2 Mini-RFQ ion source

The TRIGA-TRAP setup includes a dedicated off-line laser ablation ion source, which is designed to produce ions from dried solutions deposited on a target substrate. Furthermore, it provides carbon cluster ions, which serve as absolute mass references in Penning-trap measurements at several facilities [26–28]. This off-line laser ablation ion source is further combined with a miniaturized buffer gas-filled radio-frequency quadrupole (*mini-RFQ*) for ion trapping and cooling. The laser ablation process is driven by a pulsed, frequency-doubled Nd:YAG laser. It delivers pulses with a length of 5 ns and energies of up to 12 mJ at a wavelength of 532 nm. The laser setup is adopted from the previous laser ablation ion source as described in [29]. It includes a controllable beam attenuator based on a rotatable polarizer cube and a beam guidance and focusing system with a focal length of 0.45 m. Thereby,

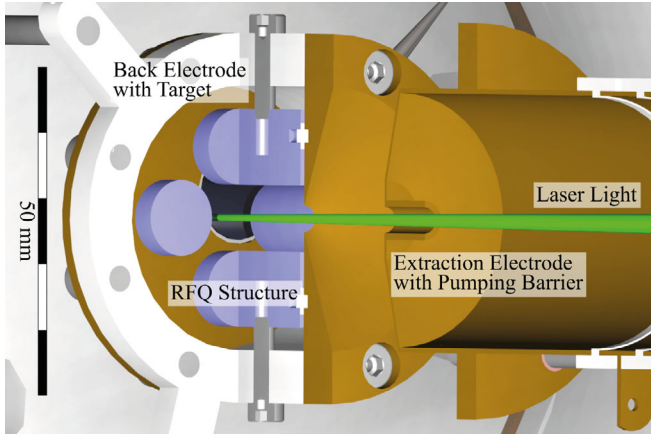


Fig. 3. Computer-rendered 3D drawing of the *mini-RFQ* ion source. The overall length, including the extraction and first focusing electrodes, is about 250 mm.

a beam spot on the target with a diameter of 0.5 mm is obtained. Typical pulse energies are set between 0.05 mJ and 0.5 mJ. By the addition of the *mini-RFQ*, the short ion bunches released by the laser pulse can be stored and cooled to the buffer-gas temperature of 300 K. Besides the decreased energy spread, the reduced phase space volume of the ion bunches ejected from the trap structure ensures an efficient transport through the beamline and injection into the Penning traps.

The *mini-RFQ* has a compact size, consisting of four rods of 40 mm length with 11.5 mm diameter and 10 mm field free region, as shown in fig. 3. The two end caps are formed by the exit electrode with a 2 mm diameter aperture and the back plate, in which the ablation target is inserted. The target is mounted on a rotary stage whose axis of revolution is positioned off-set from the quadrupole axis by 5 mm. This allows to move the laser spot along a ring-shaped area on the target and choosing a particular ablation spot position with a precision of typically 100 μm . The exit electrode of the *mini-RFQ* can be switched to a lower potential to eject the ions into the beamline, where they are accelerated to 1 keV and transported to the Penning trap.

The radiofrequency quadrupole is operated with $U_{\text{DC}} = 15 \text{ V}$ and $U_{\text{RF}} = 120 \text{ V}$ at a frequency of $\nu_{\text{RF}} = 1.077 \text{ MHz}$. For singly charged ions with $m_{\text{ion}} = 179 \text{ u}$ this creates an effective pseudopotential [30] with a depth of

$$D = \frac{q^2 U_{\text{RF}}^2}{4m_{\text{ion}} \omega_{\text{RF}}^2 r_0^2} = 6.8 \text{ V}, \quad (3)$$

whereas the ions are axially trapped by a 40 V potential well defined by the two endcaps. For the buffer-gas cooling helium gas is fed into the RFQ structure through a controllable needle valve with a flow rate of 10^{-5} mbar l/s . As the gas can only escape through the 2 mm diameter aperture in the endcap and the unsealed gaps around the target holder, this creates sufficient pressure inside the *mini-RFQ* to ensure proper cooling. The storage time was optimized by observing the width of the time-of-flight peaks in front

of the Penning trap. The minimum width, *i.e.* the smallest energy spread, was reached after 6 ms of storage. According to simulations, this situation is reached at a buffer gas pressure of approximately 10^{-3} mbar . Differential pumping, enhanced by a small tube appended to the extraction electrode, ensures vacuum pressures below 10^{-6} mbar in the subsequent part of the beamline.

2.3 Penning-trap setup

The TRIGA-TRAP setup, depicted in fig. 4 as used for off-line measurements using the *mini-RFQ*, is a low-energy beamline with ion energies of 1 keV. The ion beam produced in the *mini-RFQ*, after extraction and collimation, traverses an electrostatic quadrupole bender. This device allows selecting between ion bunches from the fission target or from the *mini-RFQ* by switching the potentials to a straight-through fashion or a 90° deflection. In addition, it enables the laser beam to be sent anti-collinearly onto the ablation target. A wire grid whose potential is switched between two values to either transmit or deflect the ion beam, acts as beam-gate 0.6 m downstream. With a transmission window of $2 \mu\text{s}$ a mass preseparation of $m/\Delta m \approx 50$ is performed before the ions enter the Penning traps.

TRIGA-TRAP is a double Penning-trap mass spectrometer inside a superconducting 7 T magnet. The first, cylindrical trap serves as a high-resolution mass filter with $m/\Delta m \geq 10^4$ by applying mass-selective buffer-gas-cooling [25]. For that purpose the radius of the magnetron motion is deliberately increased for all ions by a dipolar RF excitation. By applying a quadrupolar RF excitation near ν_c of a chosen ion species, the motion is converted to the modified cyclotron motion. This faster motion is cooled by collisions with the buffer gas and its radius is decreased, thereby centering the chosen ion species in the trap while keeping all other ion species on a larger orbit. All ions are then ejected through a 1.5 mm diaphragm, transmitting only those ions from the trap center but blocking non-centered ions. In most cases this guarantees an isotopically pure bunch, except for some exceptional cases of isobars lying very close in mass. As this is the case for ^{163}Ho and ^{163}Dy , a high sample purity is required. The cyclotron frequency measurements are performed in the second Penning trap. It features hyperbolically shaped electrodes and is positioned in the magnet bore at the location of the highest magnetic field homogeneity to ensure high-precision measurements. Its ring electrode is segmented fourfold to support the dipolar and quadrupolar RF excitations.

2.4 Measurement procedure

The determination of an atomic mass in a Penning trap is performed by measuring the free cyclotron frequency $\nu_c = qB/(2\pi m_{\text{ion}})$ of its ionized state with mass m_{ion} and charge q in a magnetic field B . To eliminate the need for

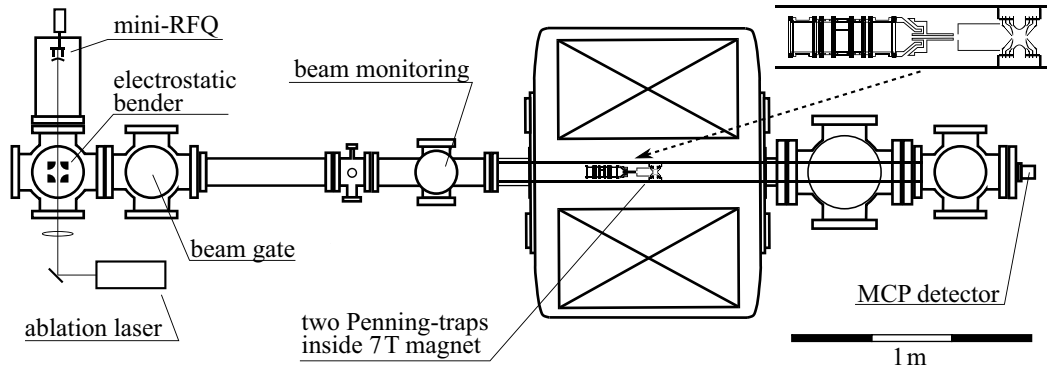


Fig. 4. Schematic drawing of the TRIGA-TRAP experimental setup. Upper-right inset: enlarged view of the Penning-trap geometry, showing the first cylindrical trap (left), the second hyperbolic trap (right) and the intermediate transfer region.

a precise magnetic field measurement, the measured cyclotron frequency is related to that of a reference ion with precisely known mass. Because the electrostatic trapping field in a Penning trap splits the ion motion into three eigenmotions—called magnetron, modified cyclotron and axial motion with the three different oscillation frequencies ν_- , ν_+ and ν_z , respectively— ν_c cannot be measured directly. At TRIGA-TRAP the determination of ν_c is therefore carried out with the so called time-of-flight ion cyclotron resonance technique (ToF-ICR) [31]. Therein, an ion bunch is captured in the Penning trap and excited with a dipolar field at the magnetron frequency ν_- to a specified radius of the magnetron motion. The motion is then converted to the modified cyclotron motion (with the same radius) by a quadrupolar π -conversion pulse with frequency ν_{rf} for all ions whose free cyclotron frequency ν_c is in resonance with ν_{rf} [32].

The conversion is probed destructively by ejecting the ions out of the trap through the magnetic field gradient of the surrounding magnet towards a microchannel plate detector. The gradient induces a gain in longitudinal kinetic energy for ions with a higher orbital moment. Thereby a conversion to the cyclotron motion is revealed by a shorter flight time to the detector. With singly charged ions in the 7 T magnetic field of TRIGA-TRAP one reaches typically a relative precision of $\delta m/m \approx 10^{-8}$. A gain in precision for the same ion storage time is possible by applying the conversion pulse in a Ramsey-type pattern of two short pulses (of larger amplitude) interspersed by a long pause. This narrows the resonance peaks and pronounces sidebands in the ToF resonance and therefore enhances the precision of the extracted cyclotron frequency [33].

From the measured cyclotron frequencies of singly charged ions of the target and reference isotope, the atomic mass and the Q -value can be derived as follows:

$$M_{\text{atom}} = \frac{\nu_{c,\text{ref}}}{\nu_{c,\text{ion}}} (M_{\text{ref}} - m_e) + m_e \quad (4)$$

$$Q_{\text{EC}} = \left(\frac{\nu_{c,\text{ref}}}{\nu_{c,\text{ion}}} - 1 \right) (M_{\text{ref}} - m_e). \quad (5)$$

Singly charged clusters of carbon $^{12}\text{C}_n^+$ serve as reference ions, as their mass is exactly $M = n \cdot 12 \text{ u}$ by definition,

neglecting the binding energy contribution of a few eV per carbon atom. Such clusters can easily be produced by laser ablation for all n up to 25 [29]. Thus, for every ion of interest with $m_{\text{ion}} \leq 300 \text{ u}$, there is a reference ion available with a mass difference of not more than 6 u. In case of the Q -value measurement, ^{163}Dy is used as direct reference to ^{163}Ho , eliminating any mass-dependent effects. The less precisely known atomic mass of ^{163}Dy is of no concern at this point, because the mass difference, *i.e.*, the Q -value, is measured directly.

The analysis of cyclotron frequency ratios eliminates the need for a precisely known magnetic field, while time, temperature, and pressure dependent drifts and fluctuations of the field still have to be considered [34]. To reduce the influence of slow changes, $\nu_{c,\text{ion}}$ and $\nu_{c,\text{ref}}$ are measured in alternation with an accumulation time of about an hour. $\nu_{c,\text{ref}}$ can then be corrected by interpolation from before and after the measurement of $\nu_{c,\text{ion}}$. Typically twenty to fifty of such cycles are performed to reach a statistical uncertainty in $\delta m/m$ below 10^{-8} .

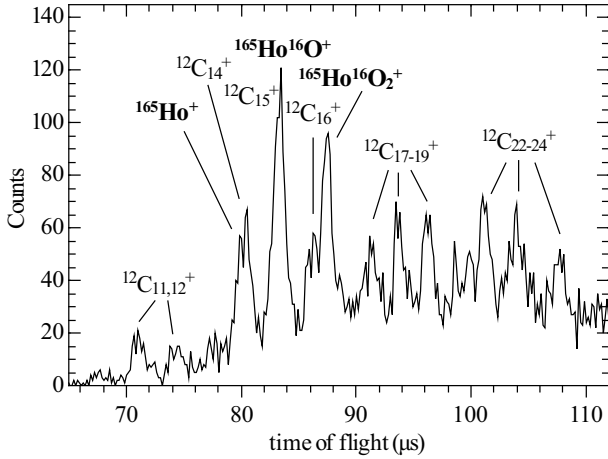
3 Results

As preparation for the mass measurements, the *mini-RFQ* performance has been characterized with stable ^{165}Ho . Using laser pulses with energies around $150 \mu\text{J}$, focused to about 0.2 mm^2 , holmium ions were produced. As is visible in the time-of-flight distribution shown in fig. 5, holmium is predominantly ionized as monoxide and dioxide ions with the monoxide being slightly more abundant ($\text{Ho}^+:\text{HoO}^+:\text{HoO}_2^+ \approx 1:2:1.6$). Dysprosium shows a similar behavior, and the measurements were performed with monoxide ions as these were most abundant. In addition, this choice has the benefit that the closest carbon cluster, in this case $^{12}\text{C}_{15}$, has a mass difference of only 1 u to $^{163}\text{Ho}^{16}\text{O}$, which decreases the impact of mass dependent systematic uncertainties in the frequency measurement. The use of the oxide ions is not disadvantageous, as the mass of ^{16}O is known to a precision of $\delta m/m = 10^{-11}$ and the binding energy of the order of a few eV can be neglected at the given measurement uncertainty level.

In the course of the measurement campaign, $^{163}\text{Ho}^{16}\text{O}$ ions were produced with a steady rate of 1–5 ions per laser

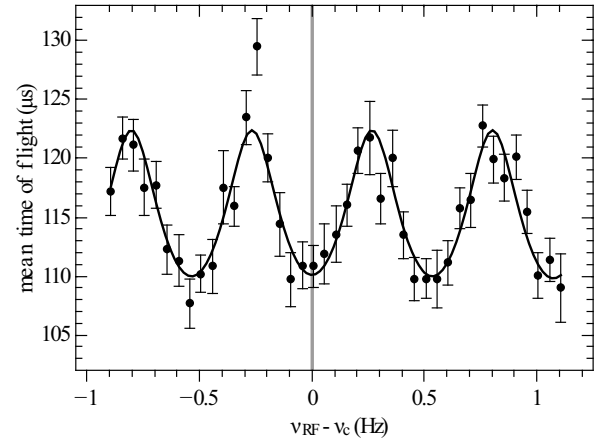
Table 1. Overview of the measured cyclotron frequency ratios including the extracted results and comparison to literature values from the Atomic-Mass Evaluation 2012 [8]. Instead of the atomic mass, the mass excess $ME = m - A u$ is given.

Target ion	Reference ion	Ratio $r = \frac{\nu_{c,ref}}{\nu_{c,ion}}$	Extracted value	Literature value
$^{163}\text{Ho}^{16}\text{O}^+$	$^{12}\text{C}_{15}^+$	0.994 020 278 3(54)	$ME(^{163}\text{Ho}) = -66379.3(9) \text{ keV}$	$-66377.3(1.9) \text{ keV}$
$^{163}\text{Dy}^{16}\text{O}^+$	$^{12}\text{C}_{15}^+$	0.994 020 264 7(48)	$ME(^{163}\text{Dy}) = -66381.7(8) \text{ keV}$	$-66379.9(1.9) \text{ keV}$
$^{163}\text{Ho}^{16}\text{O}^+$	$^{163}\text{Dy}^{16}\text{O}^+$	1.000 000 015 2(43)	$Q_{\text{EC}} = 2.5(7) \text{ keV}$	$2.555(16) \text{ keV}$

**Fig. 5.** Time-of-flight distribution of ions produced by the laser ablation ion source as recorded on the micro channel plate (MCP) in front of the Penning traps.

pulse and about 10^5 ions were detected in total. In relation to the initial sample size of $3 \cdot 10^{16}$ this corresponds to a very low efficiency. Nevertheless, comparing to the previous laser ablation ion source, the carbon cluster ion yield per laser pulse was an order of magnitude higher using the same pulse energies. The transversal confinement and the buffer-gas collisions in the *mini-RFQ* better match the produced ion bunch to the acceptance of the beamline and thus reduce the required sample size. A further improvement is possible by adjusting the sample deposition on the target to the laser trace. Currently, only a small part of the sample is exposed to the laser radiation and the majority of the sample remains on the substrate. Thus, a further reduction of the required sample size for mass measurements by an order of magnitude is achievable by correspondingly optimizing this step.

The mass measurements were performed by the ToF-ICR method with a Ramsey-type conversion [33] pulse of two 0.2 s pulses separated by 1.6 s waiting time. The resonances were sampled in a range of 2 Hz with steps of 0.05 Hz. This scan range includes the central peak and the first sideband on either side of the spectrum. To confirm the position of the central fringe a continuous excitation pulse was used in an interim measurement. 20 scans were performed before switching the ion species. Thereby each resonance typically contained 1000 to 2000 ions out of which 200 to 500 were found in events with one or two ions, to which the evaluation was constrained to limit

**Fig. 6.** Time-of-flight resonance of $^{163}\text{Ho}^{16}\text{O}^+$ recorded with a 2 s Ramsey-type excitation comprising two 0.2 s excitation pulses and 1.6 s waiting time. The solid line represents a fit of the theoretical line shape [33] to the data. The extracted cyclotron frequency is $\nu_c = 600699.982(6) \text{ Hz}$. Its uncertainty is indicated by the width of the shaded area. In total 564 events have been analyzed in this resonance.

ion-number dependent effects. From a fit of the theoretical line shape [33] to the data the cyclotron frequency was determined with an uncertainty around 0.01 Hz. As an example, one of the obtained resonances is presented in fig. 6. Frequency ratios were recorded for several combinations of targeted ion and reference ion as listed in table 1. By comparing the frequency ratios of two different combinations of carbon cluster ions, a weak mass dependence of the obtained ratios was observed. Taking the mass of $^{12}\text{C}_{14}$ as reference, the determined masses of $^{12}\text{C}_{15}$ and $^{12}\text{C}_{16}$ deviated by 1.6(1.3) keV and 3.7(1.8) keV from their nominal values. Thus, a mass dependent shift in r was determined to be $r^{-1} \Delta r / \Delta m = -8.4(3.1) \cdot 10^{-10} \text{ u}^{-1}$. Because the relevant frequency ratios are measured with a mass difference of 1 u and in case of the Q -value through a mass doublet, a shift of this magnitude has no significant impact on the measurements and no investigation upon the cause was carried out. It is however included in all calculations of the mass excesses and the Q -value.

For the determination of the atomic masses of ^{163}Ho and ^{163}Dy , 32 frequency ratios in reference to $^{12}\text{C}_{15}$ were recorded. The evaluated atomic mass of ^{163}Ho is $162.9287387(10) \text{ u}$ corresponding to a mass excess of $-66379.3(9) \text{ keV}$ and that of ^{163}Dy is $162.9287363(9) \text{ u}$ and $-66381.7(8) \text{ keV}$, respectively. The recommended values in the atomic mass evaluation [8] are in agreement within their uncertainties of 1.8 keV as listed in table 1.

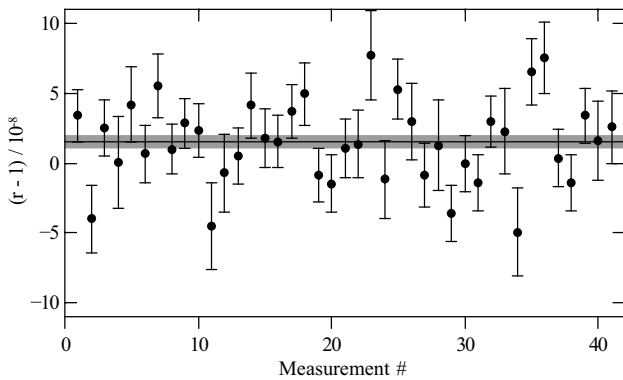


Fig. 7. Plot of the 41 recorded cyclotron frequency ratio measurements for $\nu_c(^{163}\text{Ho}^{16}\text{O}^+)$ to $\nu_c(^{163}\text{Dy}^{16}\text{O}^+)$. The solid line indicates the mean value and the shaded area its 1σ uncertainty.

These recommended values are not based on direct mass measurements, as the only direct measurement of ^{163}Dy by referencing to C_{13}H_7 has an uncertainty of 36 keV [35]. Instead, they are estimated by an adjustment calculus along an extended network of nuclides and mass differences between them. This chain of connections mostly consists of (n, γ) reactions between stable isotopes, measured with uncertainties well below 200 eV, as well as connections between elements based on β -spectroscopy or measurements of mass doublets in mass spectrometers, both with typical uncertainties around 1 keV. Based on this input data, the most precisely reported atomic masses in the range of $140 \leq A \leq 180$ are those of the gadolinium isotopes 152 to 159, with uncertainties of 1.6 keV —partly on the basis of previous measurements of our group [36]. Our measured atomic masses of ^{163}Ho and ^{163}Dy therefore represent the first mass measurements with uncertainties below 1 keV between ^{136}Xe ($ME = -86429.152(10)$ keV [37]) and ^{183}W ($ME = -46367.2(8)$ keV [38]).

The Q -value is extracted from 41 frequency ratio measurements as shown in fig. 7 with a result of $2.5(7)$ keV. This value is in agreement with the difference of $2.4(1.2)$ keV for the two measured atomic masses, but more precise due to the larger number of recorded ratios. However, this uncertainty is more than one order of magnitude larger than those reported for the calorimetric measurements.

4 Conclusion

In this work we investigated various aspects in preparation of the determination of the Q -value of the electron capture of ^{163}Ho by Penning-trap mass spectrometry. These activities included the analysis of the purity of the samples of ^{163}Ho which were produced for the ECHo project and the performance of the novel *mini-RFQ* laser ablation ion source. As the most relevant result, the direct mass measurements of ^{163}Ho and ^{163}Dy were performed. There was no indication of a ^{163}Dy contamination in the ^{163}Ho sample and the measurements could be performed with less

than 5% of the inserted $3 \cdot 10^{16}$ atoms. That allowed the successful determination of the atomic masses of ^{163}Ho and ^{163}Dy as well as the extraction of the Q -value. All results were obtained with uncertainties below 1 keV, which corresponds to a relative uncertainty of the atomic masses of $\delta m/m = 6 \cdot 10^{-9}$. An uncertainty δQ below 0.1 keV is needed in the design phase of the ECHo experiment. The number of events required to reach a 10 eV confidence level on $m(\nu_e)$ depends on the Q -value, as the relative count rate near the endpoint of the spectrum is dictated by the distance to the resonances of the N-shell capture and their inherent width. Therefore, further investigations, aiming for at least a factor of ten improvement in precision of the Q -value, are necessary. This will be addressed, *e.g.*, by using Penning-trap mass spectrometry with the *mini-RFQ* ion source and the PI-ICR method developed at SHIP-TRAP [39,40]. To reach a precision of 1 eV as required for the conclusive interpretation of the intended results of the ECHo project in terms of the neutrino mass, an ultra-high precision Penning-trap mass spectrometer like FSU-trap [17] or PENTATRAP, which is currently being set up [15,16], will be required.

We thankfully acknowledge the financial support by the Max Planck Society, the EU under ERC grant 290870 MEFUCO, the BMBF under contracts 05P12UMFN3, 05P12UMFN8 and 01DJ14002, the PRISMA Cluster of Excellence, the nuclear Astrophysics Virtual Institute (NAVI) of the Helmholtz Association, and the Helmholtz Institut Mainz. FS acknowledges support by the BMBF under contract 06MZ71661, HD acknowledges support by the Stufe 1 funding of the Johannes Gutenberg-University Mainz and SzN acknowledges support by the Alliance Program of the Helmholtz Association (HA216/EMMI).

References

1. C. Kraus, B. Bornschein, L. Bornschein, J. Bonn, B. Flatt, A. Kovalik, B. Ostrick, E. Otten, J. Schall, T. Thümmel *et al.*, Eur. Phys. J. C **40**, 447 (2005).
2. V.N. Aseev, A.I. Belev, A.I. Berlev, E.V. Geraskin, A.A. Golubev, N.A. Likhovid, V.M. Lobashev, A.A. Nozik, V.S. Pantuev, V.I. Parfenov *et al.*, Phys. Rev. D **84**, 112003 (2011).
3. KATRIN Collaboration, KATRIN design report 2004 (2005).
4. A.D. Rújula, M. Lusignoli, Phys. Lett. B **118**, 429 (1982).
5. A. Faessler, L. Gastaldo, F. Šimkovic, J. Phys. G **42**, 015108 (2015).
6. R.G.H. Robertson, Phys. Rev. C **91**, 035504 (2015).
7. A. Faessler, C. Enss, L. Gastaldo, F. Šimkovic, pre-print (2015), arXiv:1503.02282v2 [nucl-th].
8. M. Wang, G. Audi, A.H. Wapstra, F.G. Kondev, M. MacCormick, X. Xu, B. Pfeiffer, Chin. Phys. C **36**, 1603 (2012).
9. M. Lusignoli, M. Vignati, Phys. Lett. B **697**, 11 (2011).
10. P.T. Springer, C.L. Bennett, P.A. Baisden, Phys. Rev. A **35**, 679 (1987).
11. F. Gatti, P. Meunier, C. Salvo, S. Vitale, Phys. Lett. B **398**, 415 (1997).

12. P.C.-O. Ranitzsch, J.P. Porst, S. Kempf, C. Pies, S. Schäfer, D. Hengstler, A. Fleischmann, C. Enss, L. Gastaldo, J. Low, *Temp. Phys.* **167**, 1004 (2012).
13. L. Gastaldo, K. Blaum, A. Dörr, Ch.E. Düllmann, K. Eberhardt, S. Eliseev, C. Enss, A. Fässler, A. Fleischmann, S. Kempf *et al.*, *J. Low Temp. Phys.* **176**, 876 (2014).
14. K. Blaum, *Phys. Rep.* **425**, 1 (2006).
15. J. Repp, C. Böhm, J.R.C. López-Urrutia, A. Dörr, S. Eliseev, S. George, M. Goncharov, Y.N. Novikov, C. Roux, S. Sturm *et al.*, *Appl. Phys. B* **107**, 983 (2012).
16. C. Roux, C. Böhm, A. Dörr, S. Eliseev, S. George, M. Goncharov, Y. Novikov, J. Repp, S. Sturm, S. Ulmer *et al.*, *Appl. Phys. B* **107**, 997 (2012).
17. E.G. Myers, A. Wagner, H. Kracke, B.A. Wesson, *Phys. Rev. Lett.* **114**, 013003 (2015).
18. C. Smorra, T.R. Rodriguez, T. Beyer, K. Blaum, M. Block, Ch.E. Düllmann, K. Eberhardt, M. Eibach, S. Eliseev, K. Langanke *et al.*, *Phys. Rev. C* **86**, 044604 (2012).
19. C. Smorra, T. Beyer, K. Blaum, M. Block, Ch.E. Düllmann, K. Eberhardt, M. Eibach, S. Eliseev, S. Nagy, W. Nörtershäuser *et al.*, *Phys. Rev. C* **85**, 027601 (2012).
20. M. Eibach, T. Beyer, K. Blaum, M. Block, Ch.E. Düllmann, K. Eberhardt, J. Grund, S. Nagy, H. Nitsche, W. Nörtershäuser *et al.*, *Phys. Rev. C* **89**, 064318 (2014).
21. J. Ketelaer, J. Krämer, D. Beck, K. Blaum, M. Block, K. Eberhardt, G. Eitel, R. Ferrer, C. Geppert, S. George *et al.*, *Nucl. Instrum. Methods A* **594**, 162 (2008).
22. R.A. Naumann, M.C. Michel, J.L. Power, *J. Inorg. Nucl. Chem.* **15**, 195 (1960).
23. J.W. Engle, E.R. Birnbaum, H.R. Trellue, K.D. John, M.W. Rabin, F.M. Nortier, *Nucl. Instrum. Methods B* **311**, 131 (2013).
24. U. Köster, M. Günther, D. Habs, *Radiother. Oncol.* **102**, S102 (2012).
25. G. Savard, S. Becker, G. Bollen, H.J. Kluge, R. Moore, T. Otto, L. Schweikhard, H. Stolzenberg, U. Wiess, *Phys. Lett. A* **158**, 247 (1991).
26. K. Blaum, G. Bollen, F. Herfurth, A. Kellerbauer, H.-J. Kluge, M. Kuckein, E. Sauvan, C. Scheidenberger, L. Schweikhard, *Eur. Phys. J. A* **15**, 245 (2002).
27. V.V. Elomaa, T. Eronen, U. Hager, A. Jokinen, T. Kessler, I. Moore, S. Rahaman, C. Weber, J. Äystö, *Nucl. Instrum. Methods B* **266**, 4425 (2008).
28. L. Schweikhard, K. Blaum, A. Herlert, G. Marx, *Eur. J. Mass Spectrom.* **11**, 457 (2005).
29. C. Smorra, K. Blaum, K. Eberhardt, M. Eibach, J. Ketelaer, J. Ketter, K. Knuth, S. Nagy, *J. Phys. B* **42**, 154028 (2009).
30. P. Dawson, *Quadrupole mass spectrometry and its applications* (Elsevier Scientific Pub Co, Amsterdam, 1976).
31. G. Gräff, H. Kalinowsky, J. Traut, *Z. Phys. A* **297**, 35 (1980).
32. M. König, G. Bollen, H.J. Kluge, T. Otto, J. Szerypo, *Int. J. Mass Spectrom.* **142**, 95 (1995).
33. S. George, S. Baruah, B. Blank, K. Blaum, M. Breitenfeldt, U. Hager, F. Herfurth, A. Herlert, A. Kellerbauer, H.J. Kluge *et al.*, *Phys. Rev. Lett.* **98**, 162501 (2007).
34. A. Kellerbauer, K. Blaum, G. Bollen, F. Herfurth, H.J. Kluge, M. Kuckein, E. Sauvan, C. Scheidenberger, L. Schweikhard, *Eur. Phys. J. D* **22**, 53 (2003).
35. R. Demirkhanov, V. Dorokhov, M. Dzkuya, *Proceedings of the 2nd International Conference Nuclidic Masses (1964)*.
36. J. Ketelaer, G. Audi, T. Beyer, K. Blaum, M. Block, R.B. Cakirli, R.F. Casten, C. Droese, M. Dworschak, K. Eberhardt *et al.*, *Phys. Rev. C* **84**, 014311 (2011).
37. M. Redshaw, E. Wingfield, J. McDaniel, E.G. Myers, *Phys. Rev. Lett.* **98**, 053003 (2007).
38. D. Barillari, J. Vaz, R. Barber, K. Sharma, *Phys. Rev. C* **67**, 064316 (2003).
39. S. Eliseev, K. Blaum, M. Block, C. Dröse, M. Goncharov, E.M. Ramirez, D.A. Nesterenko, Y.N. Novikov, L. Schweikhard, *Phys. Rev. Lett.* **110**, 082501 (2013).
40. S. Eliseev, K. Blaum, M. Block, A. Dörr, C. Droese, T. Eronen, M. Goncharov, M. Höcker, J. Ketter, E. Ramirez *et al.*, *Appl. Phys. B* **114**, 107 (2014).